Available online at www.sciencedirect.com
ScienceDirect
Polymer 48 (2007) 5905–5916
polymer
www.elsevier.com/locate/polymer

Regulation of morphology and mechanical properties of polypropylene/poly(ethylene-*co*-propylene) in-reactor alloys by multi-stage sequential polymerization

Qi Dong [a], Xiaofeng Wang [a], Zhisheng Fu [a,b,*], Junting Xu [a,b], Zhiqiang Fan [a,b,**]

[a] *Department of Polymer Science and Engineering, Zhejiang University, Hangzhou 310027, PR China*
[b] *Key Laboratory of Macromolecular Synthesis and Functionalization, Ministry of Education, Hangzhou, 310027, PR China*

Received 12 December 2006; received in revised form 25 April 2007; accepted 24 May 2007
Available online 27 May 2007

Abstract

A series of polypropylene/poly(ethylene-*co*-propylene) (PP/EPR) in-reactor alloys were synthesized by the homopolymerization of propylene in the first stage, after that it switches to gas-phase ethylene–propylene copolymerization and gas-phase homopolymerization of propylene in a circular mode. The alloys were characterized by FTIR, DSC, PLM, TEM and SEM. Changing switch frequency had hardly any influence on the EPR content of the PP/EPR in-reactor alloys. However, as the switch frequency increased, the catalyst efficiency evidently increased. Measurement of mechanical properties shows that increasing the switch frequency has a positive effect on both the impact strength and flexural modulus. Although the content of EPR was almost similar to each other, as the switch frequency increased, the size of EPR phase decreases and the size distribution in the PP matrix trend to be more uniform that forms strong interfacial adhesion between PP phase and EPR phase. The simultaneous improvement of both impact strength and flexural modulus of the alloy can be mainly attributed to changes in its phase morphology as a result of fast circulation between homopolymerization and copolymerization.

Keywords: In-reactor alloys; Morphology; Mechanical properties

1. Introduction

The properties and applications of polyolefin have been extensively expanded by scientists and enterprisers [1–3]. Catalyst and process technology have played the major role: improvement of catalyst chemistry and control of particles morphology have allowed simplified processes, with low investment and operating costs and reduced environmental impact, as well as improved polymer properties. It has been actually for properties expansion, particularly in polypropylene but also in polyethylene, that process development has pursued the route of multi-stage process. It has been demonstrated that polymer properties could be definitely expanded by conducting polymerization in two or more successive steps, generating in each step a different polymer in terms of molecular weight, chemical composition, and crystallinity. Polypropylene/poly(ethylene-*co*-propylene) (PP/EPR) in-reactor alloy, a widely used thermal plastic material with higher toughness than PP, is just such an example. It is now mainly produced by a two-step sequential polymerization process, in which the first step is propylene homopolymerization and the second step is ethylene–propylene copolymerization. The product is a heterophasic material with PP as the continuous phase and EPR as the dispersed phase. Since the 1990s, a main progress in the production of PP/EPR in-reactor alloy has come from the use of spherical Ziegler–Natta catalyst [4–7]. PP/EPR in-reactor alloy synthesized by the catalyst is in the form of regular spherical granules, which allow higher EPR content

* Corresponding author. Department of Polymer Science and Engineering, Zhejiang University, Hangzhou 310027, PR China. Tel.: +86 571 87953754; fax: +86 571 87952400.
** Corresponding author. Tel./fax: +86 571 87952400.
E-mail addresses: fuzs@zju.edu.cn (Z. Fu), fanzq@zju.edu.cn (Z. Fan).

0032-3861/$ - see front matter © 2007 Elsevier Ltd. All rights reserved.
doi:10.1016/j.polymer.2007.05.059

without risk of reactor fouling than the polymer produced by conventional irregular Ziegler–Natta catalyst.

In previous works, we have reported the synthesis, structure and properties of PP/EPR in-reactor alloy with a superactive spherical Ziegler–Natta catalyst [8]. The in-reactor alloys show much improved impact strength, but the flexural modulus becomes lower than that of the PP homopolymer. For applications of the alloy as high-performance structural materials, it is necessary to further improve the balance between toughness and rigidity. Recently Basell developed a new process for producing PP in-reactor alloy based on multizone circulating reactor (MZCR) [2,9,10], in which the polymer granules are rapidly circulated between a reaction zone containing ethylene–propylene mixture and a reaction zone containing pure propylene. This means that during the polymerization process each polymer/catalyst particle undergoes switching between propylene homopolymerization and ethylene–propylene copolymerization for many times. It was reported that the alloy shows much improved toughness–rigidity balance than PP/EPR alloy by the conventional two-step process. However, the mechanism of this improvement is still not clear. One possibility is that polypropylene-*b*-poly(ethylene-*co*-propylene) block copolymer is formed during the rapid switching and help enhancing the properties. Another factor is spacial distribution of the rubber phase in the PP matrix. In nascent granules of PP/EPR alloy produced by a two-step process, the EPR phases are formed in one batch, which may become rather large as the copolymerization goes for long time. In a MZCR process the EPR phases may become very small because they are formed in very short reaction time. Reduction in EPR phase size may also greatly influence the properties of alloy.

In this article, we report the synthesis, morphology and mechanical properties of a series of PP/EPR in-reactor alloys, which are prepared by multi-stage sequential gas-phase homopolymerization of propylene and gas-phase ethylene–propylene copolymerization in a circular mode. By shortening the reaction time in each stage while keeping the total polymerization time unchanged, alloys resembling the PP/EPR product from a MZCR process were prepared. The experimental results show that both toughness and rigidity of the PP/EPR alloys increase as the circulation rate increases. Mechanism behind the phenomena is discussed.

2. Experimental

2.1. Synthesis of the PP/EPR alloy

The PP/EPR in-reactor alloy was synthesized in a multistage subsequential polymerization process. In the first stage, or the prepolymerization stage, the slurry polymerization of propylene was conducted in a well-stirred glass reactor for 30 min. A high yield spherical Ziegler–Natta catalyst, $TiCl_4/MgCl_2 \cdot ID$ (where ID is an internal donor), kindly donated by BRICI, SINOPEC (Beijing, China), was used in the polymerization. The catalyst had a Ti content of 3 wt%. $Al(C_2H_5)_3$ (Fluka) was used as the cocatalyst (Al/Ti = 60), and $Ph_2Si(OCH_3)_2$ was used as the external donor (Al/Si = 25). *n*-Heptane was used as the solvent. Propylene pressure in the prepolymerization stage was 1 atm and the temperature was 50 °C. A catalyst efficiency of about 30 g of PP per gram of catalyst was obtained in the prepolymerization stage. After the prepolymerization, the slurry containing the prepolymerized catalyst was transferred to a Büchiglasuster 0.5 L jacketed autoclave. Propylene was added to the autoclave to 0.6 MPa. Propylene homopolymerization was carried out for 60 min at 60 °C. At the end of this stage, propylene and solvent were removed by evacuation to 5 mmHg for 3 min, and a circular reaction mode began. An ethylene–propylene mixture of a constant composition (propylene/ethylene = 1.5) and constant pressure (0.4 MPa) was continuously supplied to the autoclave at 60 °C. After ethylene–propylene copolymerization for a designed time, the ethylene–propylene mixture was removed by evacuation to 5 mmHg for 3 min, and propylene of constant pressure (0.6 MPa) was continuously supplied to the autoclave at 60 °C. After propylene homopolymerization for a designed time, the polymerization was switch to ethylene–propylene copolymerization and subsequently propylene homopolymerization at the same conditions as above. The circular reaction mode was carried out for 80 min and illustrated in Scheme 1.

In this work, the sample EP20P60 was synthesized by ethylene–propylene copolymerization for 20 min and then propylene homopolymerization for 60 min, namely, the switch number of this sample was 1. The sample EP10P30 was synthesized by ethylene–propylene copolymerization for 10 min and then propylene homopolymerization for 30 min, namely, the switch number of this sample was 2. Analogically the switch number of EP5P15 and EP2.5P7.5 was 4 and 8, respectively. The sample EP20 was synthesized by ethylene–propylene copolymerization for 20 min without subsequent propylene homopolymerization.

2.2. Separation of random poly(ethylene-co-propylene) from the PP/EPR in-reactor alloys

About 2.5 g of every PP/EPR in-reactor alloy sample was dissolved in *n*-octane at 125 °C in 2 h, then cooled to room temperature (25 °C) in 24 h. The solution was filtered and the insoluble part was washed with *n*-heptane and dried in vacuum. Since the isotacticity of the PP catalyzed by the used spherical catalyst is more than 98 wt%, the amount of atactic PP which is solved in *n*-octane is very small. Therefore, the weight percentage of the soluble part was used as a measure of the random copolymer content in the blend.

2.3. Thermal analysis

Differential scanning calorimetry (DSC) analysis of the fractions was made on a Perkin–Elmer Pyris 1 thermal analyzer under a high purity nitrogen atmosphere. About 5 mg of each sample was sealed in an aluminum sample cell, melted at 180 °C for 5 min, and then successively annealed at 140, 130, 120, 110, 100, 90, 80, 70 and 60 °C, respectively, each

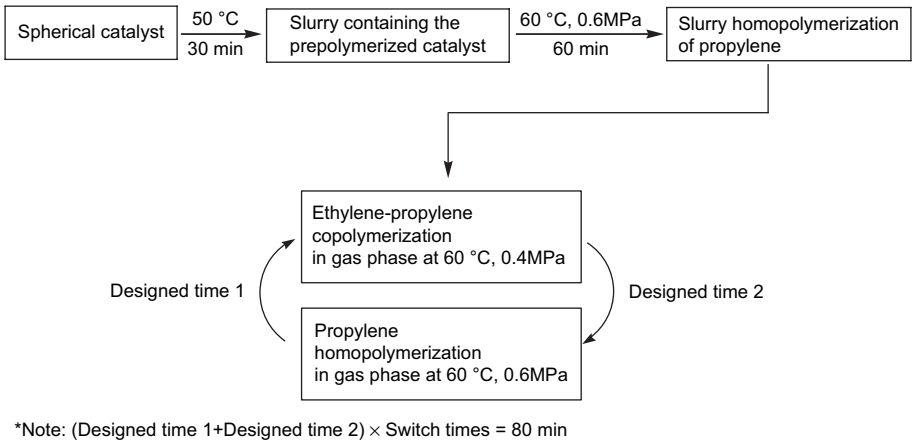

Scheme 1. Polymerization process of PP/EPR in-reactor alloy.

for 12 h. Finally the samples were cooled down to room temperature. Then the melting endotherm of the sample was recorded at a heating rate of 5 °C/min from 30 to 180 °C.

2.4. Morphology analysis

Samples for polarized light microscope observation were prepared by fusing small piece of the polymer placed between two cover glasses. After melting at 230 °C for 2 min, they were kept in quasi-isothermal state at 130 °C for 36 h. Photographs were taken using an Olympus BX51 polarized light microscope.

The morphology and dispersion state of EPR phase in the PP matrix was investigated using a transmission electron microscope (JEOL JEM-1200EX). The TEM samples were prepared as follows: strips of the polymer were prepared as described in Section 2.6, and the surface for TEM analysis were prepared by cryoultramicrotomy.

The morphology and dispersion state of EPR phase in the nascent PP/EPR in-reactor alloy particles were observed by TEM (JEOL JEM-1200EX). For TEM observation, thin sections (ca. 50–100 nm thick) prepared by ultramicrotomy of the particles were transferred onto copper grids and then stained with RuO_4 vapour for 7 h at 30 °C.

The morphology and dispersion state of EPR phase in the PP matrix were investigated using a scanning electron microscope (JSM-T20). The SEM samples were prepared as follows: strips of the polymer were prepared as described in Section 2.6, and were fractured in liquid nitrogen. The fractured surface was dipped into toluene at room temperature and etched by toluene under ultrasonic for 5 min. Then the fractured surface was coated with gold and observed by SEM.

The morphology and dispersion state of EPR phase in the nascent PP/EPR in-reactor alloy particles were observed by SEM. The SEM samples were prepared as follows: the alloy particles were mixed with epoxy resin and filled in a section of rubber tube. After solidification of the mixture, the strips of the mixture were fractured in liquid nitrogen. The fractured surface was dipped in toluene at room temperature and etched by toluene under ultrasonic for 5 min. Then the fractured surface was coated with gold and observed by SEM.

The morphology of the impact fracture surface of PP/EPR in-reactor alloys was observed by SEM. The samples for impact test were prepared as described in Section 2.6.

2.5. Porosity measurement

An AutoPore IV 9500 Porosimeter (Micromeritics Instrument Co.) was used for the mercury intrusion measurement. The apparatus has an available pressure range of 0–30,000 psi (absolute). The porosity, average pore sizes and pore size distribution of PP/EPR in-reactor alloys can be obtained from the data on intruded volume versus applied pressures. The samples were dried in vacuum at 50 °C for 12 h before the measurement.

2.6. Measurement of mechanical properties

The notched Charpy impact strength of the polymer sample was measured on a Ceast impact strength tester according to ASTM D256. The flexural modulus was measured following ASTM D790 on a Shimadzu AG-500A electronic tester. The polymer granules were heat-molded at 170 °C into sheets, which were than cut into pieces, put into a 150 × 100 × 4 mm mold, and pressed under 14.5 MPa at 180 °C for 5 min. The sample plates were then slowly cooled to room temperature in the mold. Sample strips for the tests were cut from the plate following ASTM. For each test point, five parallel measurements were made and the average values were adopted.

2.7. Fractionation with preparative TREF

Preparative temperature rising elution fractionation (TREF) apparatus was used to collect a sufficient amount of polymer fractions. About 2 g of polymer was dissolved in xylene at a concentration of 0.005 g/mL at 130 °C. This solution was deposited on an inert support, sea sand (particle diameter:

0.3–0.6 mm) packed in a steel column. The length and the internal diameter of the column were 1.0 m and 40 mm, respectively. The column was cooled to room temperature at a rate of 1.5 °C/h. Then the deposited polymer was heated stepwise and eluted with xylene at different temperatures. The polymer fractions were recovered by evaporating the xylene solvent and drying in a vacuum oven. Because a small amount of antioxidant 1010 had been added, the total recovery of polymer was slightly higher than 100 wt%.

2.8. ^{13}C NMR measurement

^{13}C NMR spectra of the fractions were measured on a Varian Mercury 300 Plus NMR spectrometer at 75 MHz. *o*-Dichlorobenzene-d_4 was used as the solvent to prepare a 20 wt% polymer solution. The spectra were recorded at 120 °C, with hexamethyldisiloxane as the internal reference. Broadband decoupling and a pulse delay of 3 s were employed. Typically, 3000 transients were collected. The ethylene content of the samples was determined on the basis of the peak area.

3. Results and discussion

3.1. Morphology and porosity of PP/EPR in-reactor alloys

Analyzed by mercury porosimeter, the parameter of porosity of sample EP20P60 and EP2.5P7.5 is shown in Table 1 and Fig. 1. It shows that the porosity of these two samples is almost the same. But there are more small pores (1–30 μm) in sample EP2.5P7.5 than that in sample E20P60.

Fig. 2 displays the TEM photographs of the morphology and dispersion state of EPR phase in the nascent PP/EPR in-reactor alloy particles. Since the EPR phase will be stained readily than the semicrystalline polypropylene matrix, it exhibits dispersed dark regions in Fig. 2. In sample EP20, as shown in Fig. 2, the transverse section of the agglomerate EPR (as indicated by the arrow) seemed to be strips (ca. 1.2 × 0.2 μm) which indicated that EPR did not finely disperse in the PP matrix. The situation in sample EP20P60 was similar to that of sample EP20, except that the phase size of agglomerate EPR in the former was little smaller than that in the latter. But in samples EP10P30, EP5P15 and EP2.5P7.5, as the switch frequency increased, the phase size of EPR became smaller and the shape of the agglomerate EPR tended to be globular. In sample EP2.5P7.5, the EPR phase was closely globular and less than 0.6 μm. It indicated that, in the nascent PP/EPR in-reactor alloy particles, the dispersion of the rubber phase became more and more uniform as the switch frequency increased.

Table 1
The parameter of porosity compare of the samples

Sample	EP20P60	EP2.5P7.5
Sample weight (g)	0.4051	0.4715
Total intrusion volume (mL/g)	0.3720	0.3431
Total pore area (m^2/g)	15.611	16.02
Median pore diameter (volume) (μm)	75.3753	49.9075
Median pore diameter (area) (μm)	0.0103	0.0104
Average pore diameter (4V/A) (μm)	0.0953	0.0857
Bulk density at 0.53 psia (g/mL)	0.6548	0.6639
Apparent skeletal density (g/mL)	0.8656	0.8597
Porosity (%)	24.3581	22.78
Stem volume used (%)	39	42

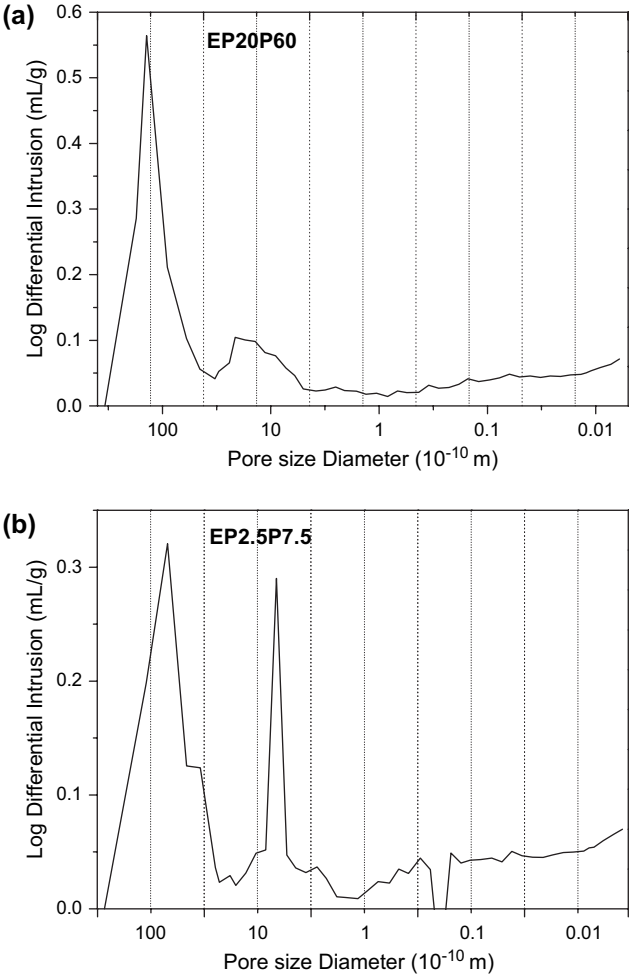

Fig. 1. Pore diameter distribution of samples: (a) EP20P60 and (b) EP2.5P7.5.

Fig. 3 displays the TEM photographs of the morphology and dispersion state of EPR phase in the PP/EPR in-reactor alloy strips. In samples EP20 and EP20P60, the phase size and shape of EPR were irregular. In samples EP10P30 and EP5P15, the shape of the agglomerate EPR tended to be globular and the phase size of EPR became smaller (most of them were less than 1 μm). Especially in sample EP2.5P7.5, the interface between PP phase and EPR phase became ambiguous which illustrated that the compatibility between PP phase and EPR phase was very well.

Fig. 4 displays the SEM photographs of the cryogenically fractured surface of nascent PP/EPR in-reactor alloy particles etched by toluene. The EPR phase, which is soluble in toluene at room temperature, was removed by toluene etching and small cavities were left on the surface. In sample EP20, the fractured surface looked rather smooth, besides some large

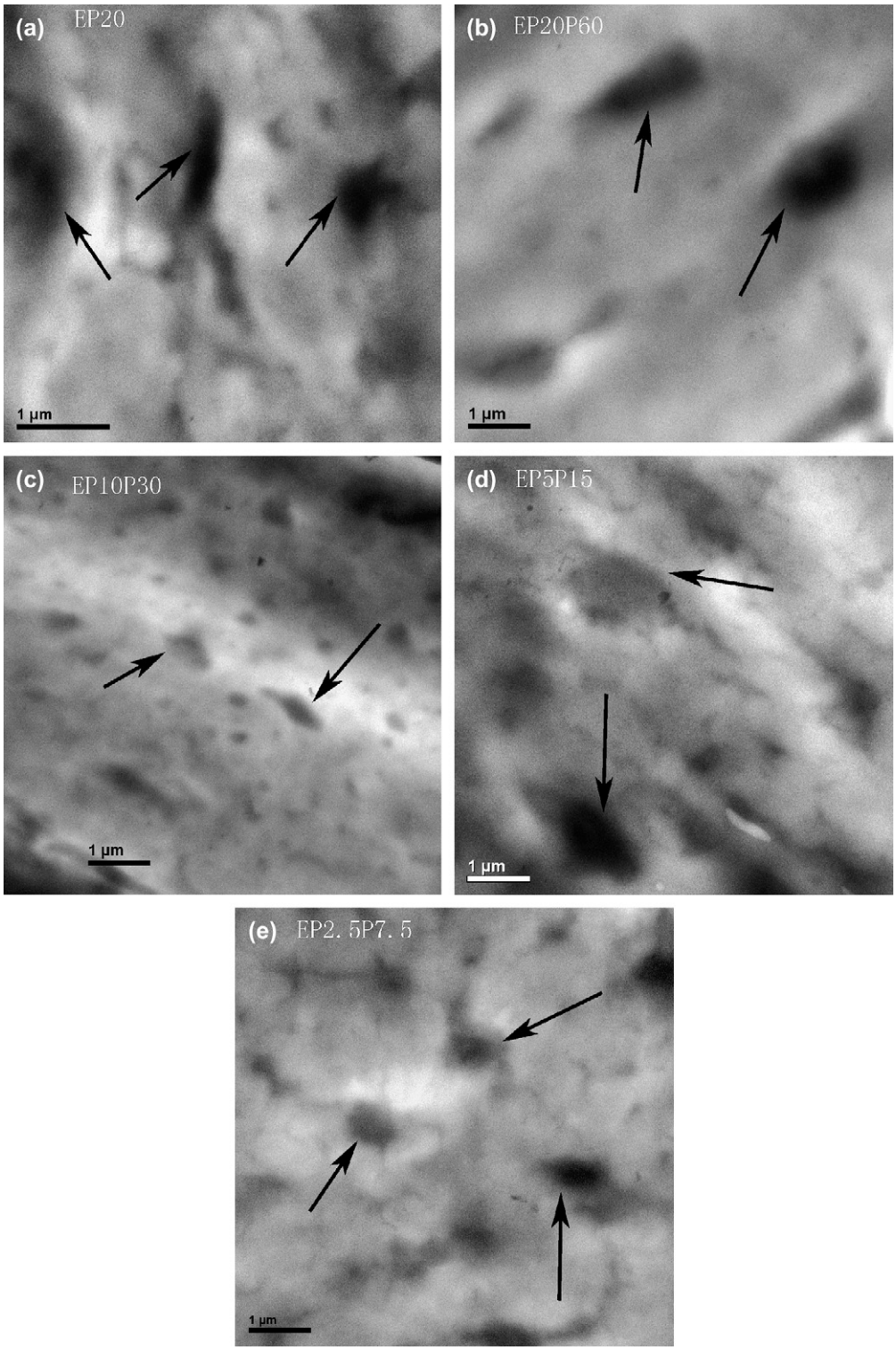

Fig. 2. TEM photographs of the morphology and dispersion state of EPR phase in the nascent PP/EPR in-reactor alloy particles: (a) EP20; (b) EP20P60; (c) EP10P30; (d) EP5P15; (e) EP2.5P7.5.

holes or hollows that are larger than 5 μm. There were almost no cavities smaller than 2 μm in the view. It could be said that the rubber phase in sample EP20 was not uniformly dispersed in the PP matrix, as most of the cavities were larger than 2 μm. As the switch frequency increased, more small cavities on the fractured surface became observable. When the switch frequency was raised to 8 times (sample EP2.5P7.5), the shape of the small cavities tended to be globular indicating the dispersion of the rubber phase became rather uniform.

Fig. 5 displays the SEM photographs of the cryogenically fractured surface of PP/EPR in-reactor alloy strips etched by

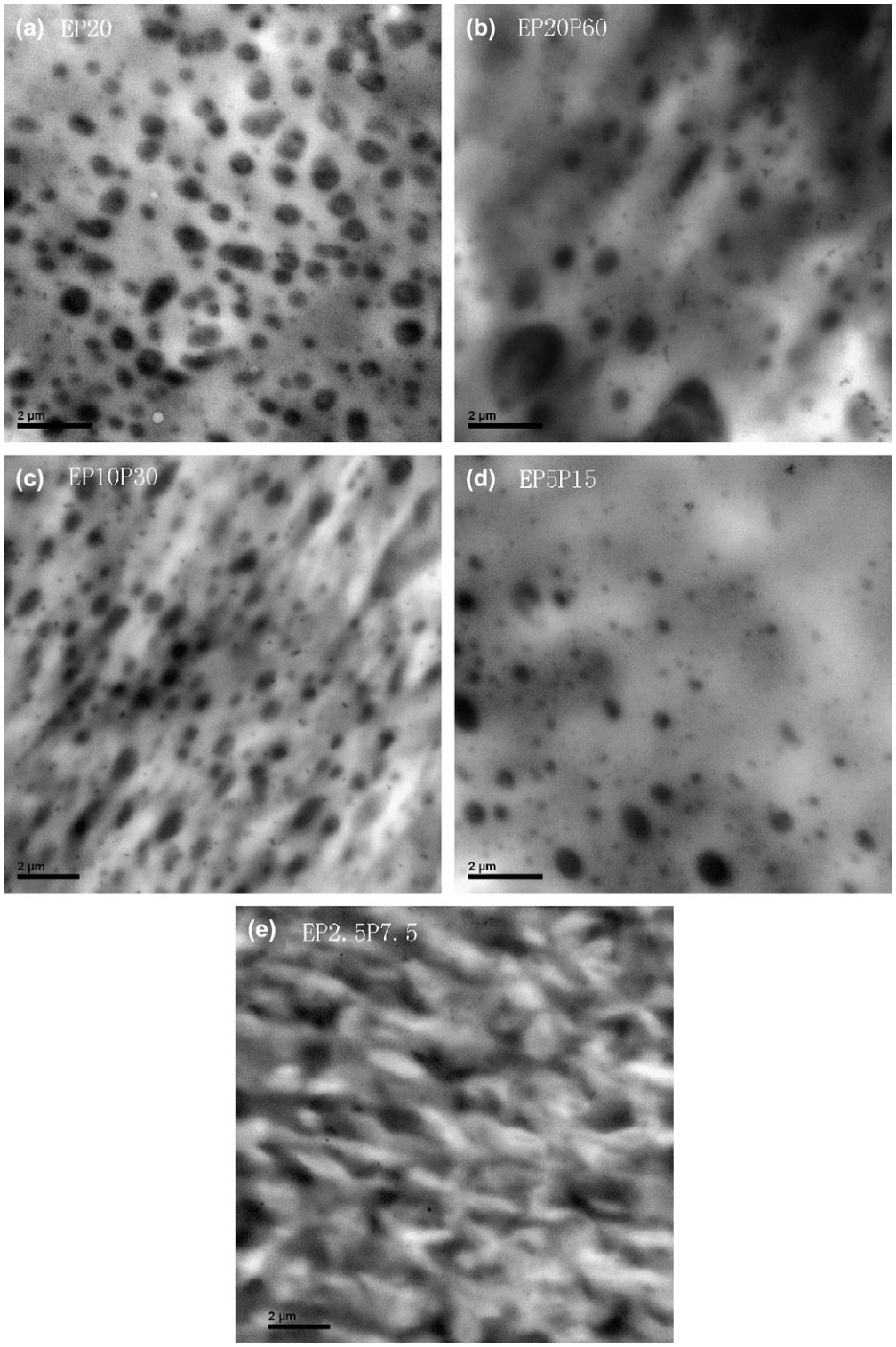

Fig. 3. TEM photographs of the morphology and dispersion state of EPR phase in the PP/EPR in-reactor alloy strips: (a) EP20; (b) EP20P60; (c) EP10P30; (d) EP5P15; (e) EP2.5P7.5.

toluene. In the pictures, biphasic structure can be clearly seen. In sample EP20, the cavities' dispersion was rather disordered. In sample EP10P30, the cavities' dispersion was more uniform than that of sample EP20, with an average cavity diameter less than 1 μm. When the switch frequency was raised to 8 times (sample EP2.5P7.5), the average diameter of the cavities was markedly decreased to about 0.5 μm and the cavities' dispersion became more uniform. It shows that as switch frequency increases, the compatibility between PP phase and EPR phase increases. Only a limited number of studies on PP/EPR or high impact PP morphology have been published [11–14], and because of the complexity of the problem, no

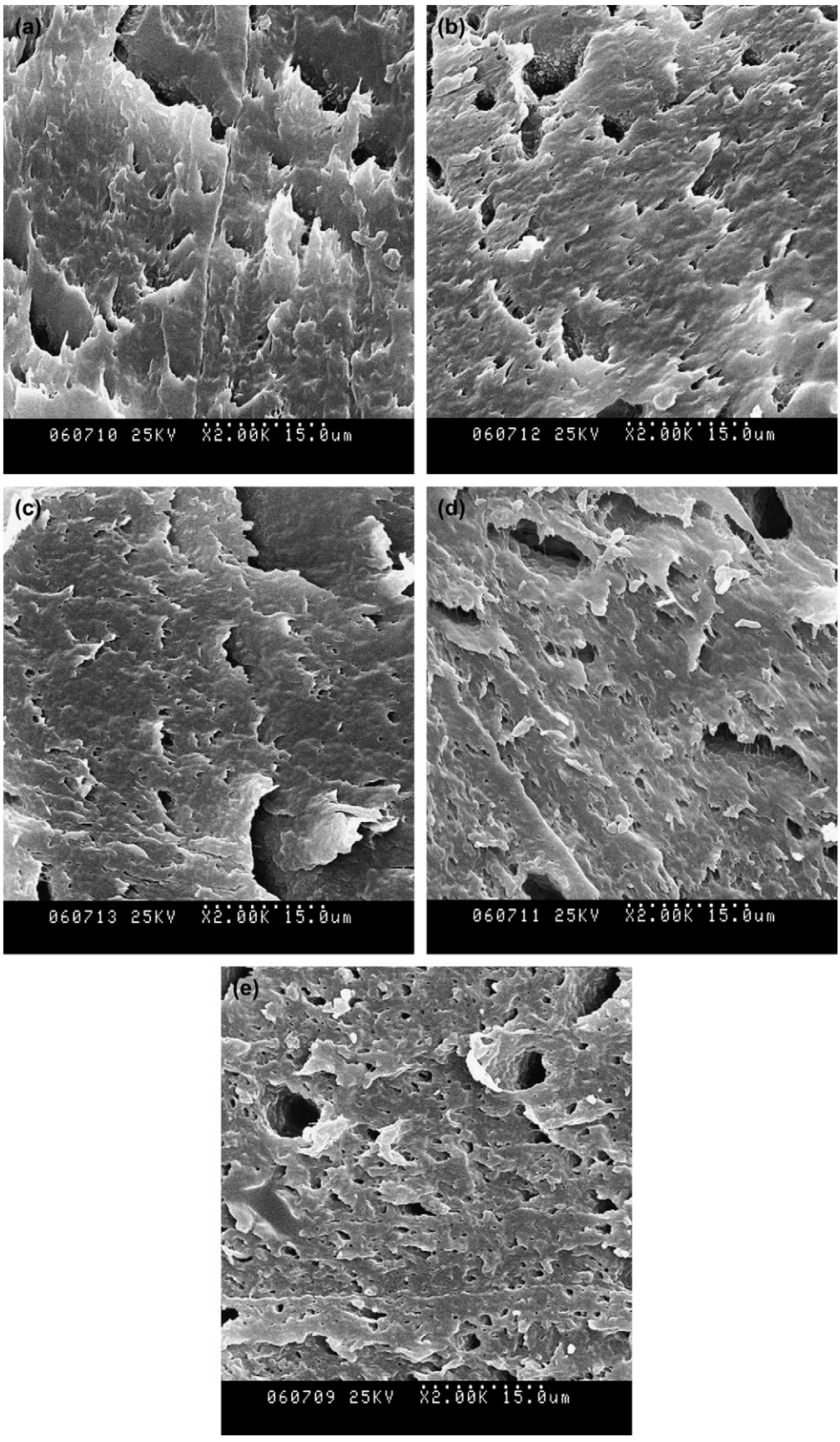

Fig. 4. SEM photographs of cryogenically fractured surface of the nascent PP/EPR in-reactor alloy particles etched by toluene at 50 °C: (a) EP20; (b) EP20P60; (c) EP10P30; (d) EP5P15; (e) EP2.5P7.5.

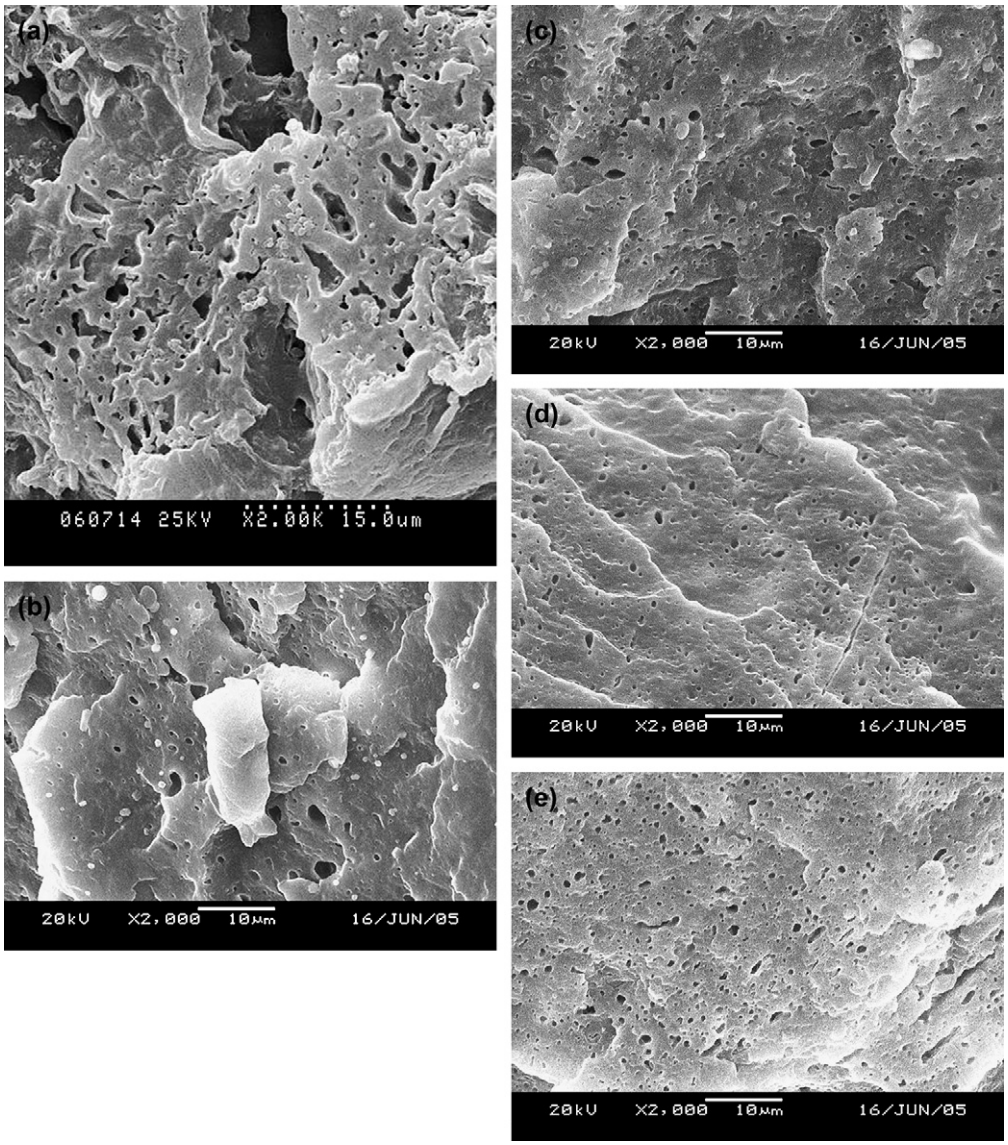

Fig. 5. SEM photographs of fractured surface of the PP/EPR in-reactor alloys after etched by toluene at 50 °C: (a) EP20; (b) EP20P60; (c) EP10P30; (d) EP5P15; (e) EP2.5P7.5.

model satisfied completely the growth and morphology of these particles. Recently Chen et al. [15] reported that the iPP particle exhibits a tertiary architecture consisting of many secondary subglobules with the diameter of from several to hundreds of microns. The subglobule in turn is formed by a great deal of primary globules ca. 100 nm in diameter. The large macropores between the subglobules and the finely distributed micropores within the subglobule constitute a network of pore inside the iPP particle. There is a fine distribution of catalyst fragments in the iPP particle, which are active for the copolymerization of ethylene and propylene to occur. The ethylene–propylene comonomers can diffuse into the macro- and micropores and copolymerize on the catalyst active sites located on the periphery of the pores, forming the elastomer phase inside. Based on this consideration, a hypothetical model of morphology of the PP/EPR in-reactor alloy granules prepared by multi-stage sequential polymerization is shown in Scheme 2. In Scheme 2, white section represents PP phase, grey section represents EPR phase and the black dot represents the active center. The shortcomings of the three-stage processes (sample EP20P60) can be seen in the model. After ethylene–propylene copolymerizing for a long time (20 min), tiny pores in the primary globules of PP homopolymer were largely filled with the copolymer. In the subsequent homopolymerization of propylene, the diffusion limitation will prevent propylene monomer from contacting with the active center. As a result, the catalyst efficiency of sample EP20P60 was low and the rubber phase became larger and more disordered. However, in sample EP2.5P7.5, as each copolymerization took place only for a short time (2.5 min), only small amount of copolymer will be formed around the active center. As a result, the tiny pores in the primary globules, acting as the channel for propylene monomer to contact with the active center, would not be occluded. Hence, the subsequent homopolymerization of propylene could be carried out effectively and show high catalyst efficiency. Due to the insertion of crystalline

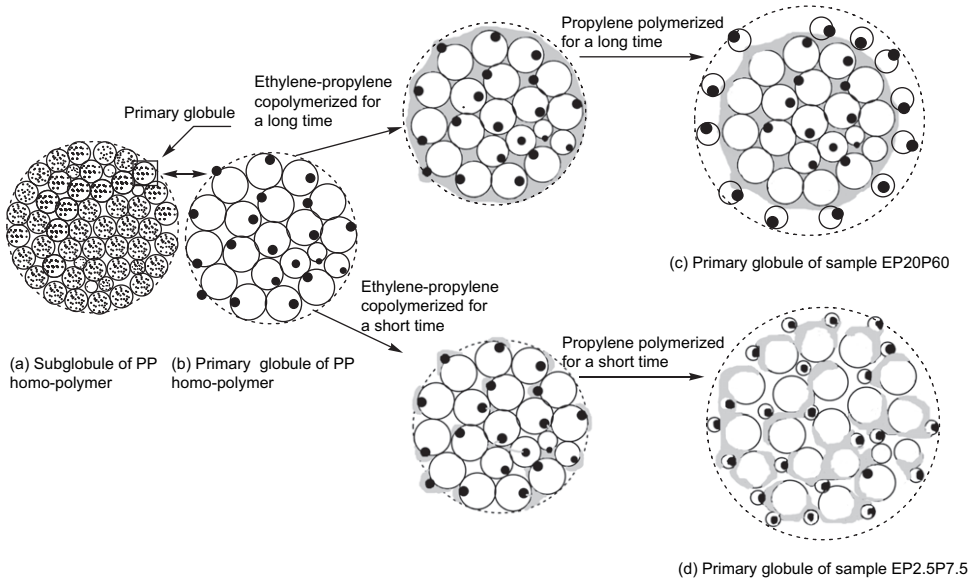

Scheme 2. The model of morphologies of the PP/EPR granules.

PP into the rubbery EPR phase, most of the tiny pores (1–10 μm) can be remained.

3.2. Influence of switch frequency on the composition and polymerization rate of PP/EPR in-reactor alloys

In a previous study [16], we found that there are many factors, such as monomer pressure and feed ratio of ethylene–propylene mixture, affect the copolymerization rate strongly. As the amount of ethylene in the ethylene–propylene mixture increased, the EPR content in the product increased. To avoid such effect, in the copolymerization stage, the ethylene–propylene mixture was supplied at a constant ratio and at constant temperature and pressure. As shown in Table 2, increasing the switch frequency had a strong effect on the catalyst efficiency, but hardly on the EPR content in the product. The catalyst efficiency can reflect the polymerization rate. As the switch frequency increased, the polymerization rate increased. However, EPR content in all the products were about 16 wt%. This phenomenon can be explained by the diffusion limitation to polymerization in the particle. As the polymer particle consists of primary globule [15], the tiny pores between the primary globules in the PP granule will be gradually filled with ethylene–propylene copolymer as the copolymerization proceeded, and the monomers had to diffuse through the solid polymer layer before reaching the active sites. In sample EP20P60, after a long time (20 min) of copolymerization most of the tiny pores will be filled with copolymer, and in the subsequent stage it limited the monomer to contact with the active sites. However, in sample EP2.5P7.5, copolymerization continues only for a short time (2.5 min) and only a small amount of ethylene–propylene copolymer will be filled into the tiny pores between the primary globules. In the subsequent stage, propylene monomer will be able to diffuse through the tiny pores easily. After a short time (7.5 min) of propylene homopolymerization, more tiny pores may be formed or the original tiny pores may be enlarged, owing to the insertion of crystalline PP into the soft EPR phase. As a result, the polymerization rate of sample EP20P60 was much lower than that of sample EP2.5P7.5.

3.3. Thermal analysis

The DSC heating scanning curves of the *n*-octane insoluble part of the samples are shown in Fig. 6. The melting curve of all four samples obviously shows two melting peaks at 167 and 175 °C. It means that the *n*-octane insoluble part of all four samples was mainly composed of pure PP. In the range of 60–120 °C there are several weak endothermic peaks. They are mainly caused by the melting of the PE lamella of relatively short thickness [17].

Table 2
Influence of switch frequency on the catalyst efficiency and mechanical properties of the PP/EPR in-reactor alloys

Sample	Switch frequency (times)	Catalyst efficiency (gPP/gcat·h)	*n*-Octane soluble part (wt%)	Impact strength (kJ/m^2)	Flexural modulus (Mpa)
EP20P60	1	899.6	15.8	3.9	770.68
EP10P30	2	1016.2	17.8	11.1	852.61
EP5P15	4	1026.3	15.3	11.6	856.38
EP2.5P7.5	8	1316.7	17.5	13.6	915.68

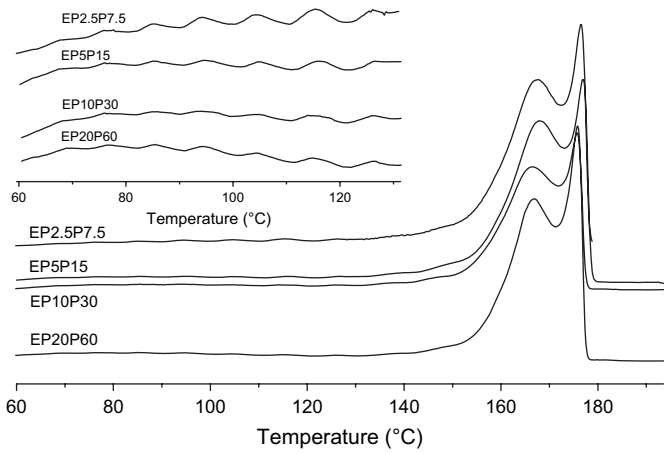

Fig. 6. DSC curves of the annealed *n*-octane insoluble part of the samples EP20P60, EP10P30, EP5P15 and EP2.5P7.5.

3.4. Crystalline morphology

The crystalline morphology of the isothermal crystallized PP/EPR in-reactor alloys was studied by polarized light microscope. As shown in Fig. 7, switch frequency markedly influenced the crystalline morphology. In the alloy sample with only one switch, relatively large spherulites of PP were found, but when the switch number was increased to 8, many small and irregular spherulites can be observed. This means that the crystallization of PP was more strongly influenced by the copolymer in sample EP2.5P7.5. This caused significant phase mixing between the PP phase and the EPR phase as indicated by the very small size of the latter [as shown in Figs. 3(e) and 5(e)]. Such high degree of phase mixing could hinder the formation of large and regular spherulites.

3.5. Chain structure of PP/EPR in-reactor alloys

Fig. 8 shows the results of TREF fractionation of the samples EP20P60 and EP2.5P7.5. Although there is difference in the amounts of the fractions eluted higher than 100 °C, the distribution of fractions eluted lower than 100 °C was almost the same for the two samples. As characterized by ^{13}C NMR, the content of propylene unit of samples EP20P60 and EP2.5P7.5 was 92.1 and 90.4 mol%, respectively. ^{13}C NMR spectra of the fractions from sample EP2.5P7.5 were recorded. The spectrum of the 25 °C fraction is a typical spectrum of a random ethylene–propylene copolymer. This random copolymer was mainly produced in the stage of ethylene–propylene copolymerization. In the spectra of fractions eluted at temperature lower than 100 °C (e.g., 60 and 80 °C fractions), there was a strong signal of long PE sequences. Meanwhile, there are several peaks corresponding to the PPP sequence, such as $P_{\beta\beta}$ at 20.0 ppm, $T_{\beta\beta}$ at 26.8 ppm, and $S_{\alpha\alpha}$ at 44.6 ppm, meaning that there were long PP segments in the polymer chain. The peaks at 35.7–36.0 ($S_{\alpha\delta}$ and $S_{\alpha\gamma}$), 31.3 ($T_{\delta\delta}$), 25.4 ($S_{\beta\delta}$), 22.9 ($S_{\beta\beta}$), and 18.1 ppm ($P_{\delta\delta}$) indicate that there were also sequences such as PPEE, EEPEE, and PEP in the polymer chain [18]. This shows that the fractions eluted at lower than 100 °C were segmented copolymers of ethylene and propylene. The ^{13}C NMR spectra of the fractions eluted

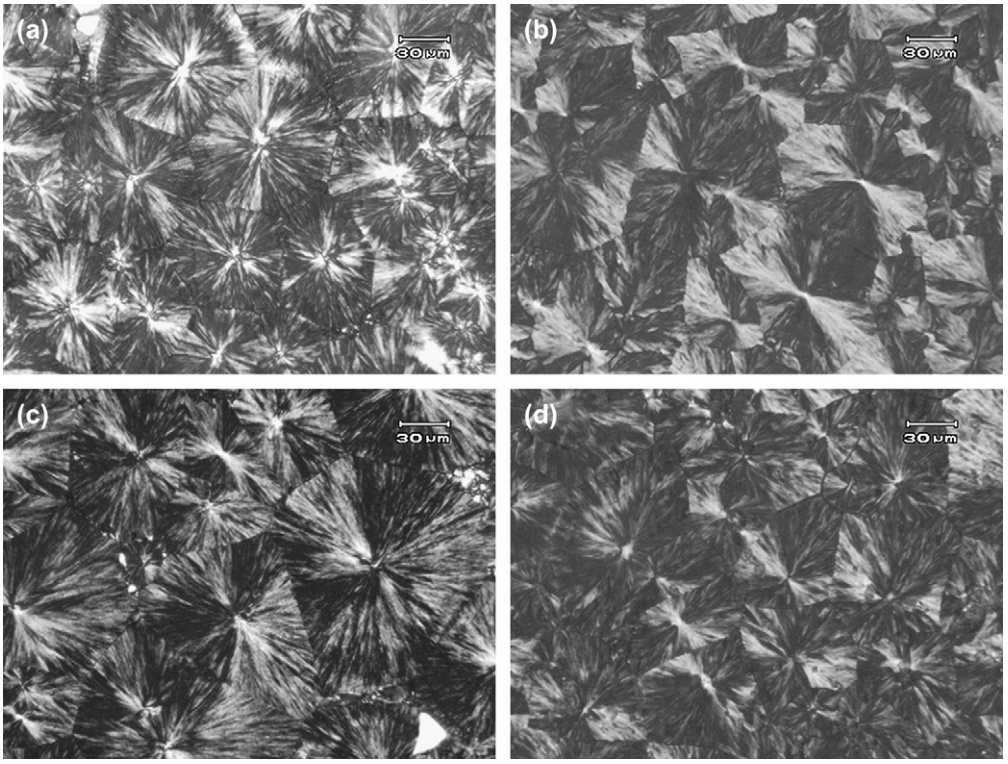

Fig. 7. PLM photographs of the isothermally crystallized PP/EPR in-reactor alloy samples: (a) EP20P60; (b) EP10P30; (c) EP5P15; (d) EP2.5P7.5.

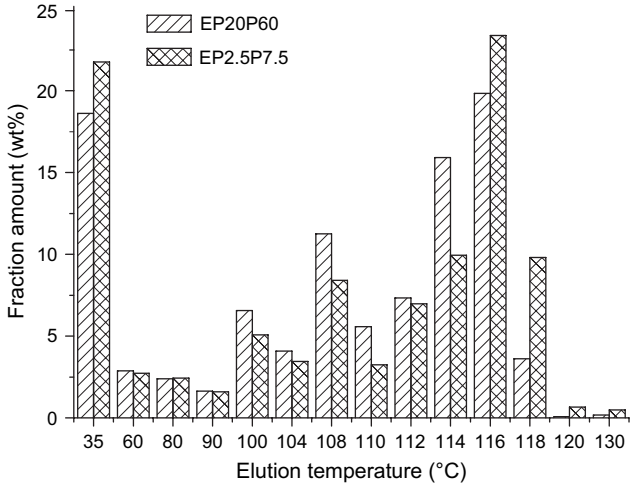

Fig. 8. Fraction distribution of samples EP20P60 and EP2.5P7.5.

at higher than 100 °C show that they are pure polypropylene. The results of ^{13}C NMR and TREF show a clear map of the chain structure and structure distribution of the PP/EPR in-reactor alloys synthesized by multi-stage sequential polymerization. Pure PP constituted more than 70 wt% of the alloy. The content of ethylene–propylene random copolymer was about 20 wt% of the alloy, and the remaining fraction was ethylene–propylene segmented copolymer. As the two samples have similar content of these three components of alloys, we can conclude that the chain structure and structure distribution of the alloys are scarcely influenced by the switch frequency.

3.6. Mechanical properties of the PP/EPR in-reactor alloys

Properties of polymer alloy are mainly dependent on their phase structure under given measurement conditions,

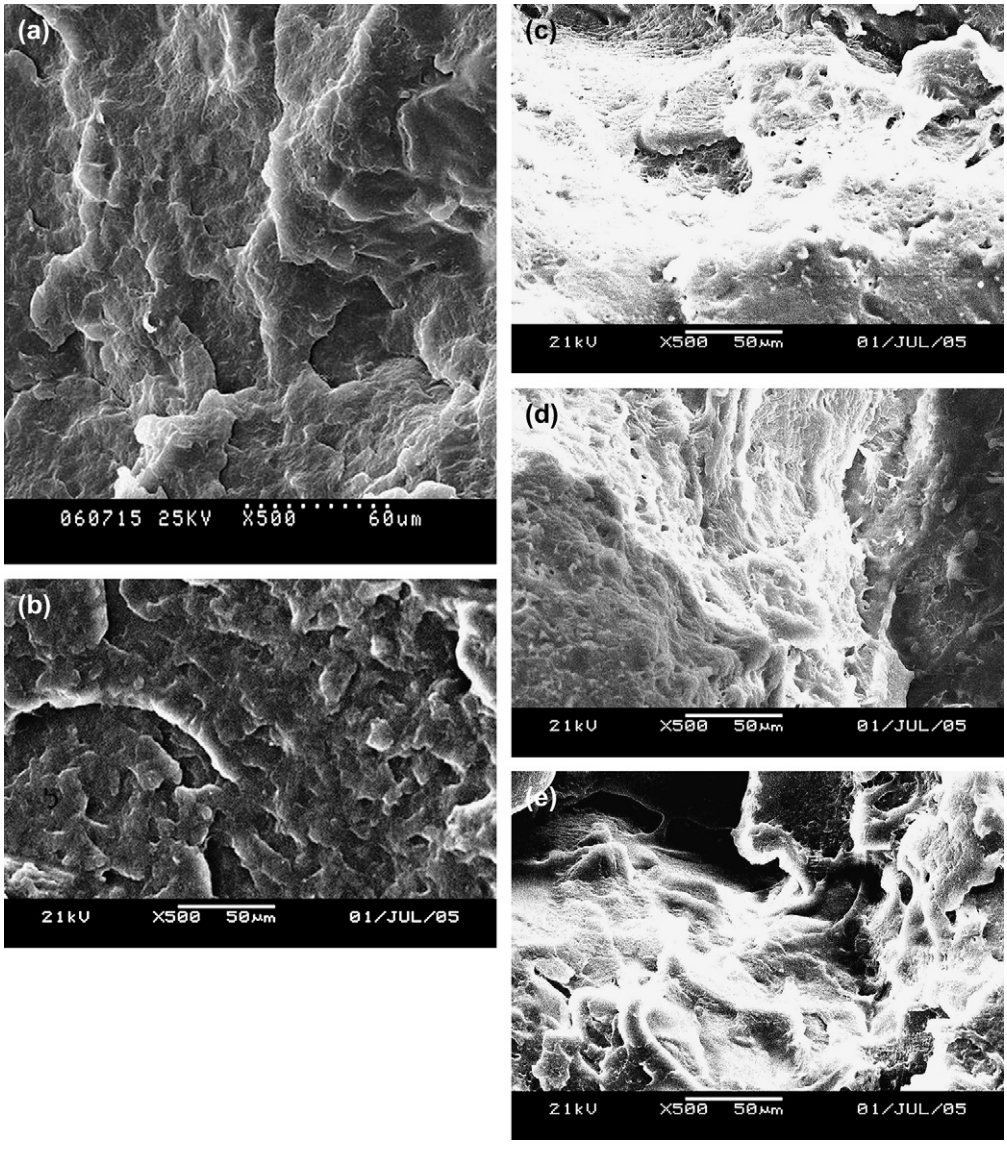

Fig. 9. SEM photographs of the impact fracture surfaces of PP/EPR in-reactor alloys fractured at room temperature (28 °C): (a) EP20; (b) EP20P60; (c) EP10P30; (d) EP5P15; (e) EP2.5P7.5.

especially the interfacial morphological structure between the matrix and the dispersed phase. The morphology of PP-rubber blends is closely related to the compatibility between the continued phase and the dispersed phase [19]. Wu [20] demonstrated a direct relationship among chain structure, phase morphology, and toughness in polymer–rubber blends: the dispersed rubber toughens a polymer–rubber blend mainly by promoting energy dissipation of the matrix, and the toughening efficiency correlates with morphology of the rubber phase and chain structure of the matrix. The shape, content, size, and size distribution of dispersed phase are important factors determining the toughening effect of the rubber phase, which are related to the micro-morphological structure of the materials. Jang et al. [21] collected information on rubber particle size using transmission electron microscopy (TEM) and computer-aided image analysis, and observed the effects of rubber particle size on crazing in the PP matrix. The results showed that PP blends with smaller rubber particles are tougher and more ductile than those with larger particles. On the other hand, the larger the rubber particle size, the easier it will be for the cavitation to take place [22]. Therefore, there is a best particle size for optimum toughening effect. In general, besides the properties of the matrix, the toughening mechanism of polymer–rubber blends has a close relation with interfacial adhesion between the filler and the matrix. For a blend system with strong interfacial adhesion, multiple crazing is favored, while for a blend system with poor interfacial adhesion, shear yielding is favored [23].

To see the effects of switch frequency and morphology on mechanical properties of PP/EPR in-reactor alloys, we have measured the notched Charpy impact strength and flexural modulus of the samples synthesized with different switch frequency (see Table 2). As shown in Table 2, both the impact strength and the flexural modulus of the samples increased as the switch number was increased. It is clear that PP/EPR in-reactor alloys synthesized by multi-stage sequential polymerization have good balance between toughness and rigidity. It is well known that the morphology of a material's impact fracture surface is closely related to its impact property. Fig. 9 shows the SEM pictures of the impact fracture surface of PP/EPR in-reactor alloys. The impact fracture surface of samples EP20 and EP20P60 (Fig. 9(a) and (b)) is quite smooth, reflecting their poor toughness. In contrast, Fig. 9(b)–(d) shows ductile and coarse fashion of the fractured surfaces. Moreover, on the impact fracture surface of sample EP10P30 (Fig. 9(c)) there were many disordered globule cavities formed by pulling EPR phase out from the surface. Comparatively, there were much less globule cavities on the impact fracture surface of sample EP5P15 (Fig. 9(d)), and its size of globule cavities were smaller. However, there were almost no globule cavities on the impact fracture surface of sample EP2.5P7.5 (Fig. 9(e)), but there were strip-like protrusions on the surface. Such fine pleats have not been found in PP/EPR blends prepared by mechanical blending. This phenomenon should be directly related to the excellent compatibility between PP phase and EPR phase that markedly improved the mechanical properties of PP/EPR in-reactor alloys.

4. Conclusions

In this research work, we used the process of multi-stage sequential polymerization to improve the morphology and mechanical properties of PP/EPR in-reactor alloys. A series of PP/EPR in-reactor alloys with good balance between toughness and rigidity were synthesized by spherical Ziegler–Natta catalyst in a circular reaction mode. Although increasing the switch frequency does not change the chain structure and structure distribution of the alloys in a detectable level, the size of EPR phase decreases and its size distribution becomes more uniform when the switch frequency is increased. The simultaneous improvement of both impact strength and flexural modulus of the alloy can be mainly attributed to changes in its phase morphology as a result of fast circulation between homopolymerization and copolymerization.

Acknowledgements

Support by the Special Funds for Major State Basic Research Projects (grant no. 2005CB623804) and the National Natural Science Foundation of China (grant no. 20474053) are gratefully acknowledged.

References

[1] Cecchin G, Morini G, Pelliconi A. Macromol Symp 2001;173:195.
[2] Covezzi M, Mei G. Chem Eng Sci 2001;56:4059.
[3] Fernandes FAN, Lona LMF. J Appl Polym Sci 2004;93:1042.
[4] Galli P. Prog Polym Sci 1994;19:959.
[5] Galli P, Vecellio G. Prog Polym Sci 2001;26:1287.
[6] Fu ZS, Fan ZQ, Zhang YZ, Xu JT. Polym Int 2004;53:1169.
[7] Fu ZS, Xu JT, Zhang YZ, Fan ZQ. J Appl Polym Sci 2005;97:640.
[8] Fan ZQ, Zhang YQ, Xu JT, Wang HT, Feng LX. Polymer 2001;42:5559.
[9] Santos JL, Asua JM, de la Cal JC. Ind Eng Chem Res 2006;45:3081.
[10] Fernandes FAN, Lona LMF. J Appl Polym Sci 2004;93:1053.
[11] Debling JA, Ray WH. J Appl Polym Sci 2001;81:3085.
[12] Cecchin G, Marchetti E, Baruzzi G. Macromol Chem Phys 2001;202:1987.
[13] Mckenna T, Bouzid D, Matsunami S, Sugano T. Polym React Eng 2003;11:177.
[14] Tanem BS, Kamfjord T, Augestad M, Lovgren TB, Lundquist M. Polymer 2003;44:4283.
[15] Chen Y, Chen Y, Chen W, Yang DC. Polymer 2006;47:6808.
[16] Zhang YZ, Fan ZQ, Liu Z, Zhang YQ, Feng LX. Acta Polym Sin 2002;432.
[17] Fu ZS, Fan ZQ, Zhang YQ, Feng LX. Eur Polym J 2003;39:795.
[18] Tritto I, Fan ZQ, Locatelli P, Sacchi MC, Camurati I, Galimberti M. Macromolecules 1995;28:3342.
[19] Yang D, Zhang B, Yang Y, Fang Z, Sun G. Polym Eng Sci 1984;24:612.
[20] Wu S. Polym Eng Sci 1990;30:753.
[21] Jang BZ, Uhlmann DR, Vander SJB. Polym Eng Sci 1985;25:643.
[22] van der Wal A, Gaymans RJ. Polymer 1999;40:6067.
[23] Liang B, Li Y, Xie GH. Macromol Rapid Commun 1996;17:193.